Bioconjugate Chemistry

Article

pubs.acs.org/bc

Controlled Assembly of SNAP−PNA−Fluorophore Systems on DNA Templates To Produce Fluorescence Resonance Energy Transfer

Zahra Gholami[†] and Quentin Hanley*

School of Science and Technology, Nottingham Trent University, Clifton Lane, Nottingham NG11 8NS, United Kingdom

ABSTRACT: The SNAP protein is a widely used self-labeling tag that can be used for tracking protein localization and trafficking in living systems. A model system providing controlled alignment of SNAP-tag units can provide a new way to study clustering of fusion proteins. In this work, fluorescent SNAP−PNA conjugates were controllably assembled on DNA frameworks, forming dimers, trimers, and tetramers. Modification of peptide nucleic acid (PNA) with the O^6-benzyl guanine (BG) group allowed the generation of site-selective covalent links between PNA and the SNAP protein. The modified BG−PNAs were labeled with fluorescent Atto dyes and subsequently chemo-selectively conjugated to SNAP protein. Efficient assembly into dimer and oligomer forms was verified via size exclusion chromatography (SEC), electrophoresis (SDS-PAGE), and fluorescence spectroscopy. DNA-directed assembly of homo- and heterodimers of SNAP−PNA constructs induced homo- and hetero-FRET, respectively. Longer DNA scaffolds controllably aligned similar fluorescent SNAP−PNA constructs into higher oligomers exhibiting homo-FRET. The combined SEC and homo-FRET studies indicated the 1:1 and saturated assemblies of SNAP−PNA−fluorophore:DNA formed preferentially in this system. This suggested a kinetic/stoichiometric model of assembly rather than binomially distributed products. These BG−PNA−fluorophore building blocks allow facile introduction of fluorophores and/or assembly directing moieties onto any protein containing SNAP. Template-directed assembly of PNA-modified SNAP proteins may be used to investigate clustering behavior both with and without fluorescent labels, which may find use in the study of assembly processes in cells.

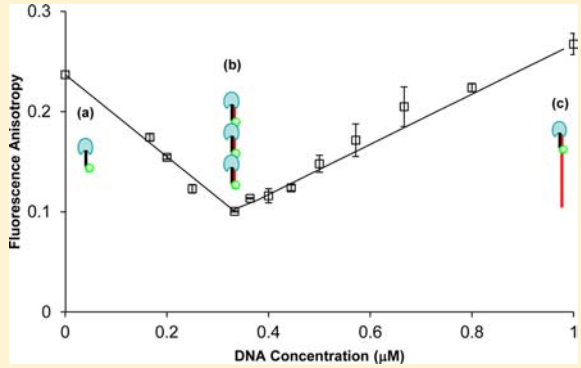

INTRODUCTION

Studying inducible aggregation such as that occurring in cell membrane proteins requires a model system featuring controlled assembly. Biological macromolecules such as DNA and proteins are currently being studied as building blocks of self-assembled nanoarchitectures due to their size and unique recognition capabilities.[1] Furthermore, self-assembled DNA−protein conjugates can be used as template-controlled systems for spatially arraying other molecules with increased relative accuracy and programmability.[1−5] The programmable hybridization of nucleic acid provides a framework to design nanoscale assemblies.[6−15]

Peptide nucleic acid (PNA) provides excellent control properties over a self-assembled system including better stability than DNA duplexes, even for short sequences, and higher mismatch sensitivity. Moreover, its neutral net charge allows for tuning the structural and electrostatic characteristics through using other amino acids instead of glycine. Modification with other amino acids is easily accessible through synthesis or conjugation methods and should allow good control over the dynamics of assembly.[7,16] The unique properties of PNA gave good results for programmable assembly of nanoparticles,[4,17] which can be potentially extended to clustering of other molecules such as proteins.

PNA tag-encoding technology has been used to assemble libraries of small molecules,[18,19] carbohydrates,[20] peptides,[21−23] and protein fragments[24,25] into organized microarrays through hybridization to DNA. Because of the compatibility with standard peptide chemistry, PNA is the only oligonucleotide tag that can be cosynthesized with small molecules by solid-phase synthesis. It allows PNA-encoded libraries synthesized by the split and mix method to be decoded in one step.[26,27]

Recently, the self-assembly of PNA−α-HER2 antibody Fab fragments conjugated into homodimer, heterodimer, and higher order multimers of defined composition, valency, and controlled geometry was reported. The tetrameric assembly showed enhanced activity in comparison with that of the parent monocolonal antibody. Site-specific modification of the antibody using a genetically encoded unnatural amino acid allowed precise control of PNA−antibody conjugation.[9,25,28]

The oligomeric self-assembly of PNA-tagged carbohydrates with controlled topology has also been reported.[20,29] Scheibe and Seitz used the hybridization of PNA−sugar conjugates with complementary DNA as a powerful tool to create a well-defined spatial arrangement of carbohydrates that can be applied for precise spatial screening of carbohydrate−lectin interactions.[30−33]

Received: July 18, 2014
Revised: September 3, 2014
Published: September 5, 2014

   dx.doi.org/10.1021/bc500319p | *Bioconjugate Chem.* 2014, 25, 1820−1828

Site-specific labeling of protein with synthetic molecules such as PNA can provide an intriguing and versatile tool to study the function and structure of proteins and their behavior in clustering forms. The noninvasive imaging of the dynamics of proteins in living systems can be obtained by fusion of proteins of interest with protein or peptide tags as a means for subsequent attachment of a fluorophore or other biophysical probes.[34,35]

Self-labeling protein tags such as the SNAP protein provide high specificity and selectivity.[35] Furthermore, a wide range of colors with unique photophysical properties can be obtained by subsequent modification of self-labeling tags with organic fluorophores, which make them a great method to localize and study fusion protein behavior in living systems.[36−38]

The SNAP tag is a 19−20 kDa self-labeling tag that was developed by mutation of the DNA repair protein O^6-alkylguanine-DNA alkyltransferase (AGT). The labeling of a SNAP-tag is based on the specific reaction of benzylguanine (BG) derivatives with a reactive cysteine residue of AGT, leading to the irreversible formation of a covalent bond.[37−45] BG derivatives can be generated via a range of conjugation procedures, allowing specific labeling to a wide variety of molecules including PNA (Scheme 1), and the ligand attached to BG does not have an impact on the rate of reaction between SNAP and the BG derivative.[38,46−48]

Scheme 1. Coupling of BG−PNA−Atto Dyes to the SNAP Protein To Produce a Thioether Bond between Cysteine of SNAP and Benzyl Linker of Modified Construct

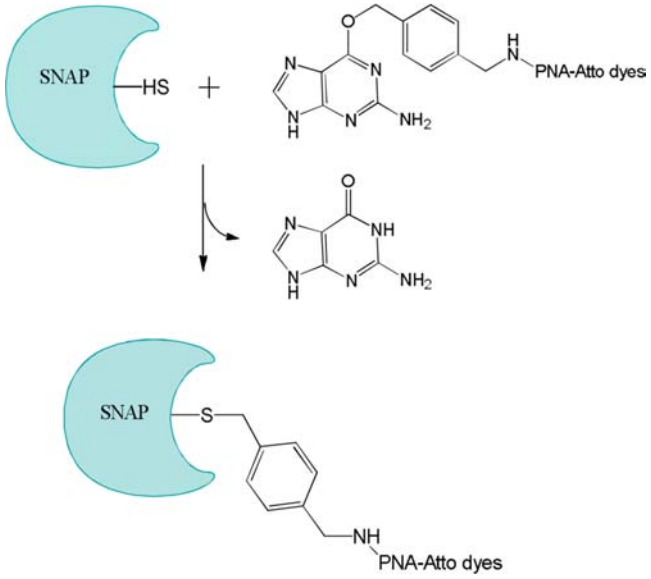

SNAP-tag labeling has been used extensively in in vitro and in vivo experiments. Examples include localization and trafficking of a fusion protein in the cell membrane, labeling of antibody fragments, designing fluorescent biosensors, controlling yeast transcription, and visualization of metabolite signaling.[49−56]

In our previous work, a well-defined system for studying controlled protein assembly based on fluorescent protein−PNA conjugates demonstrated control over the exact composition and structure of an inducibly assembled system following addition of a DNA template.[5] Moreover, it allowed fundamental insights into the behavior of proteins in self-assembled architectures by observing the photophysical behavior of assembled FPs.[57] Here, the combination of the unique recognition characteristics of PNA with the wide application of SNAP tag has been used to provide versatile, well-defined units to create programmed self-assembled protein systems. The induced assembly by DNA templates has been studied through fluorescence resonance energy transfer (FRET) techniques. Four DNA scaffolds were used as frameworks to create dimeric and oligomeric forms (Scheme 2), creating heterodimers and a range of homo-oligomers exhibiting FRET, which was verified with fluorescence spectroscopy.

Scheme 2. Assembly of SNAP−PNA1−Fluorophore Constructs into Dimeric and Higher Oligomeric Forms[a]

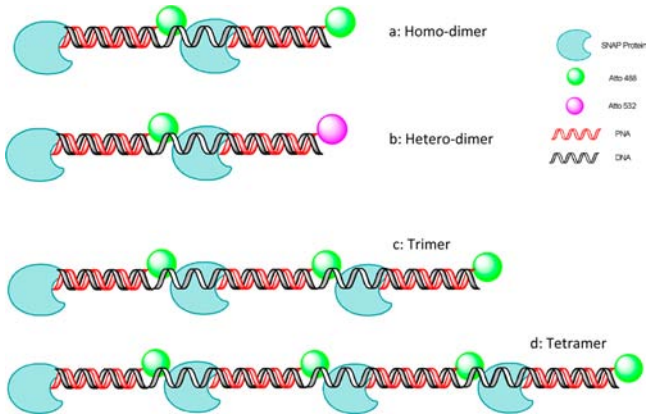

[a](a) Assembly of two SNAP−PNA1−Atto488 constructs into a homodimer (DNA1-dimer), (b) assembly of SNAP−PNA2−Atto532 and SNAP−PNA1−Atto488 into a heterodimer (DNA2-dimer), (c) assembly of three SNAP−PNA1−Atto488 constructs into a trimeric form (DNA3-trimer), and (d) assembly of four SNAP−PNA1−Atto488 molecules into a tetramer (DNA4-tetramer).

RESULTS AND DISCUSSION

Synthesis of BG−PNA−Fluorophore Conjugates. Fluorescent SNAP−PNA conjugates were prepared by coupling of PNA to an O^6-benzylguanine (BG) derivative and subsequently labeling with Atto dyes. This allows the SNAP protein to react specifically with the BG group attached to a fluorescent PNA. After transferring the benzyl group of the BG to the cysteine residue in the active site of the SNAP, the fluorescent PNA is covalently conjugated to the SNAP. This gives a handle for directed assembly and allows visualization of the protein.

The maleimide derivative of BG underwent reaction with the thiol group of cysteine at the N-terminus of the PNA1 and PNA2 sequences, forming stable thioether bonds[58] in the presence of TCEP at 4 °C overnight at pH 7.2.

The production of BG−PNA conjugates was assessed by MALDI-TOF MS and reverse-phase HPLC (RP-HPLC). Mass spectrometry of conjugates showed peaks at 2492 Da (calculated, 2494 Da) and 2514 Da (calculated, 2516) related to BG−PNA1 and BG−PNA2, respectively. The RP-HPLC showed that the peak related to PNA1 at 24.32 min completely disappeared after conjugation to BG−maleimide, indicating efficient conversion to BG−PNA1. The data showed peaks at 23.83 min for both BG−PNA1 and BG−PNA2.

The BG−PNAs were subsequently labeled with fluorescent dyes. Because of their high photostability and brightness, Atto

dx.doi.org/10.1021/bc500319p | Bioconjugate Chem. 2014, 25, 1820−1828

dyes (Atto488: λ_{ex}, 501 nm and λ_{em}, 523 nm; Atto532: λ_{ex}, 532 nm and λ_{em}, 553 nm) were chosen to label the BG−PNA conjugates. Labeling targeted the primary amine group of a C-terminal lysine on PNA with NHS-esters of the Atto dyes. The reaction with NHS-ester derivatives was performed in pH 7.2 phosphate buffer at room temperature for 1 h in the dark. The RP-HPLC data showed single peaks for the Atto488 derivative (23.8 min) when monitoring at 501 nm and for the Atto532 (23.7 min) derivative at 532 nm. Mass spectral analysis of the products revealed peaks at 3066 Da (calculated, 3065 Da) and 3147 Da (calculated, 3148 Da), indicating production of BG−PNA1−Atto488 and BG−PNA2−Atto532 with good conversion of unlabeled BG−PNA1 and BG−PNA2 to BG−PNA1−Atto488 and BG−PNA2−Atto532 conjugates, respectively.

Coupling of BG−PNA−Fluorophore to SNAP Protein. The coupling of BG−PNA−Atto constructs to SNAP was performed by mixing 2 equiv of the modified PNA1−BG−Atto488 and PNA2−BG−Atto532 constructs with 1 equiv of SNAP in phosphate buffer, pH 7.4, after 2 h incubation in dark at 37 °C. The reaction proceeded by producing a thioether bond between the cysteine residue of SNAP and the benzyl linker of the modified constructs (Scheme 1). The final products were purified subsequently by dialysis to remove unreacted compounds.

Mass spectrometry confirmed the production of SNAP−PNA1−Atto488 and SNAP−PNA2−Atto532 conjugates at 22 900 kDa (calculated, 22 896 kDa) and 22 980 kDa (calculated, 22 976 kDa), respectively. SDS-PAGE of SNAP−PNA−Atto dye conjugates exhibited a single band at 23 kDa, indicating complete conversion of SNAP protein to the conjugated forms (Figure 1), and SEC-HPLC yielded peaks eluting at the same time (9.4 min) for both the SNAP−PNA−Atto488 and SNAP−PNA−Atto532 conjugates. The SEC-HPLC data also showed that using a higher ratio of construct to SNAP and longer incubation time did not have strong effects on conjugation; however, performing the reaction at room temperature decreased the coupling efficiency by about 80%.

Figure 1. SDS-PAGE results for SNAP−PNA−Atto conjugates. The bands related to purified SNAP and to SNAP−PNA−Atto488 and SNAP−PNA−Atto532 conjugates are at 20, 23, and 23 kDa, respectively.

Assembly of Fluorescent SNAP−PNA in Dimer and Higher Oligomer Forms. The DNA1 and DNA2 sequences contained two complementary sections engineered to assemble SNAP−PNA1−Atto488 into homodimers and SNAP−PNA1−Atto488 and SNAP−PNA2−Atto532 into heterodimers, respectively (Scheme 2a,b). DNA3 and DNA4 were designed to demonstrate assembly of higher oligomers and consisted of three and four complementary parts for SNAP−PNA1−Atto488, respectively (Scheme 2c,d).

SDS-PAGE analysis was carried out after 5 min heating of each sample at 90 °C. Heating resulted in melting of PNA:DNA assemblies followed by partial reassembly of units. In the case of a 2:1 ratio of SNAP−PNA1−Atto 488:DNA1, three distinct bands were observed (23, 27, and 50 kDa) corresponding to SNAP−PNA1−Atto488 (monomer), monomer:DNA1, and dimer:DNA1, respectively. Similarly, mixing a 1:1:1 ratio of SNAP−PNA1−Atto488:SNAP−PNA2−Atto532:DNA2 resulted in the same three bands (23, 27, and 50 kDa) related to SNAP−PNA1−Atto488 and SNAP−PNA2−Atto532 (both as monomer), monomer:DNA2, and dimer:DNA2 of both SNAP−PNA1−Atto488 and SNAP−PNA2−Atto532 hybridized to DNA2 (Figure 2).

Under the same conditions, a 3:1 ratio of SNAP−PNA1−Atto488:DNA3 produced four distinct bands (23, 31, 54, and 77 kDa), which were assigned to SNAP−PNA1−Atto488 (monomer), monomer:DNA3, dimer:DNA3, and trimer:DNA3, respectively. Kinetic effects on assembly, as might be expected from Scheme 1, are indicated by the band

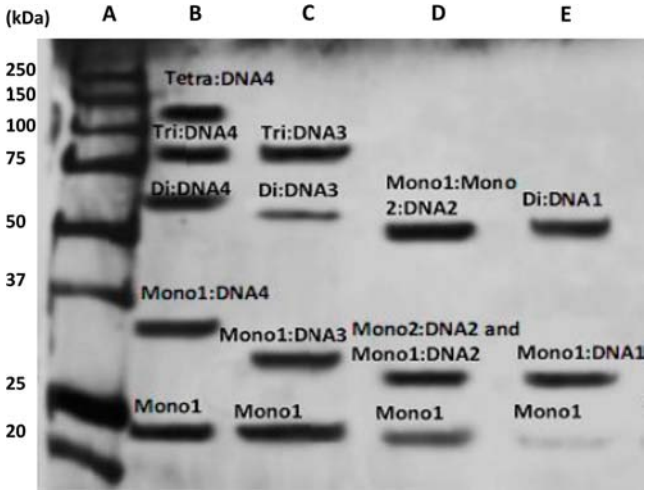

Figure 2. SDS-PAGE results for SNAP−PNA−Atto monomers assembled in dimers and oligomers using different DNA templates (A−D). (A) Standard protein ladder. (B) Tetramer formation; 4:1 ratio of SNAP−PNA1−Atto488:DNA4 showed five bands at 23, 34, 57, 80, and 103 kDa, respectively, related to SNAP−PNA1−Atto488 monomer or Mono1, monomer:DNA4 (Mono1:DNA4), dimer:DNA4 (Di:DNA4), trimer:DNA4 (Tri:DNA4), and tetramer:DNA4 (Tetra:DNA4). (C) Trimer formation; 3:1 ratio of SNAP−PNA1−Atto488:DNA3 showed 4 bands at 23, 31, 54, and 77 kDa, respectively, related to SNAP−PNA1−Atto 488 monomer or Mono1, monomer:DNA3 (Mono1:DNA3), dimer:DNA3 (Di:DNA3), and trimer:DNA3 (Tri:DNA3). (D) Heterodimer formation; 1:1:1 ratio of SNAP−PNA1−Atto488:SNAP−PNA3−Atto532:DNA2 showed 3 bands at 23, 27, and 50 kDa, respectively, related to both monomers of SNAP−PNA1−Atto488 and SNAP−PNA3−Atto532 (Mono1 and Mono2), monomer:DNA2 (Mono1:DNA2 and Mono2:DNA2), and dimer:DNA2 (Mono1:Mono2:DNA2) consisting of both SNAP−PNA1−Atto488 and SNAP−PNA3−Atto532 hybridized to DNA2. (E) Homodimer formation; 2:1 ratio of SNAP−PNA1−Atto488:DNA1 resulted in 3 bands at 23, 27, and 50 kDa, respectively, related to SNAP−PNA1−Atto488 monomer or Mono1, monomer:DNA1 (Mono1:DNA1), and dimer:DNA1 (Di:DNA1).

corresponding to dimer:DNA3 having relatively less intensity than that of the other bands. A 4:1 ratio of SNAP−PNA1−Atto488:DNA4 resulted in five bands (23, 34, 57, 80, and 103 kDa) corresponding to SNAP−PNA1−Atto488 (monomer), monomer:DNA4, dimer:DNA4, trimer:DNA4, and tetramer:DNA4, respectively (Figure 3). The tetrameric system did not show clear signs of kinetic effects in the gel; however, there was evidence of this in the anisotropy data (cf. lower panel of Figure 5).

SEC-HPLC of a solution containing a 2:1 ratio of SNAP−PNA1−Atto488:DNA1 indicated a new peak at 8.6 min when observed at 214 and 501 nm, which was attributed to the efficient assembly of the homodimer on the DNA1 scaffold (Figure 3). Similarly, when SNAP−PNA1−Atto488 and SNAP−PNA3−Atto532 were assembled as a heterodimer on the DNA2 scaffold, a new peak appeared at 8.6 min at 501 nm (Atto488) and at 532 nm (Atto532). A titration of DNA1 with an increasing amount of SNAP−PNA1−Atto488 indicated a gradual decrease of the peak related to free SNAP−PNA1−Atto488 monomer, which reached zero at a 2:1 ratio of SNAP−PNA1−Atto488 to DNA1 while the peak related to DNA1:dimer reached its highest, showing the complete conversion of monomer units to template assembled dimers.

The solutions featuring 3:1 SNAP−PNA1−Atto488:DNA3 and 4:1 of SNAP−PNA1−Atto488:DNA4 ratios showed additional peaks at 8.16 min (timer) and 7.79 min (tetramer) at both 501 and 214 nm wavelengths. The peaks indicated assembly in trimer form on the DNA3 scaffold and tetramer form on the DNA4 scaffold (Figure 3). Titrations of these solutions with an increasing amount of SNAP−PNA1−Atto488 showed a gradual decrease of the monomer peak, which eventually reached zero at 3:1 (SNAP−PNA1−Atto488:DNA3) and 4:1 (SNAP−PNA1−Atto488:DNA4) ratios while both peaks of trimer:DNA3 and tetramer:DNA4 reached their maximum. This behavior was attributed to the efficient formation of trimer and tetramer assemblies.

SEC-HPLC analysis of the distribution of products during titration of the DNA3 systems did not follow predictions based on the binomial distribution (Figure 3, bottom panel). Specifically, the products of the reaction favored products containing a single SNAP−PNA construct and the saturated constructs. This suggested that reaction of the 1:1 SNAP−PNA:DNA species was rate-limiting. Similar results were seen for the tetrameric assembly on DNA4.

Photophysical Studies of Fluorescent SNAP−PNA Assemblies. Hetero-FRET System. To study the effects of template-directed assembly on the fluorescent properties of the SNAP−PNA molecules, DNA2 template (5′-TGCATGGATC-GTTACT-3′) was used as a framework to make heterodimers. The DNA2 template consisted of sequences directing a 1:1 assembly of SNAP−PNA1−Atto488 and SNAP−PNA2−Atto532 separated by a distance of approximately 3.7 nm, which is ∼0.57 of the Förster distance for this energy transfer pair (R_0 = 6.4 nm) (Scheme 2b). This intensity for a solution containing a 1:1 ratio of SNAP−PNA1−Atto488:DNA2 exhibited fluorescence characteristic of Atto488 when excited at 501 nm. Addition of SNAP−PNA2−Atto532 to form a 1:1:1 assembly of SNAP−PNA1−Atto488:SNAP−PNA20Atto532:DNA2 resulted in a reduction in Atto488 (donor) fluorescence and sensitized emission of Atto532 (acceptor), reaching a maximum at 553 nm (Figure 4). The average FRET efficiency of a set of four replicates of the 1:1:1 assembly was 93 ± 2%, which confirmed the efficient assembly of two monomer

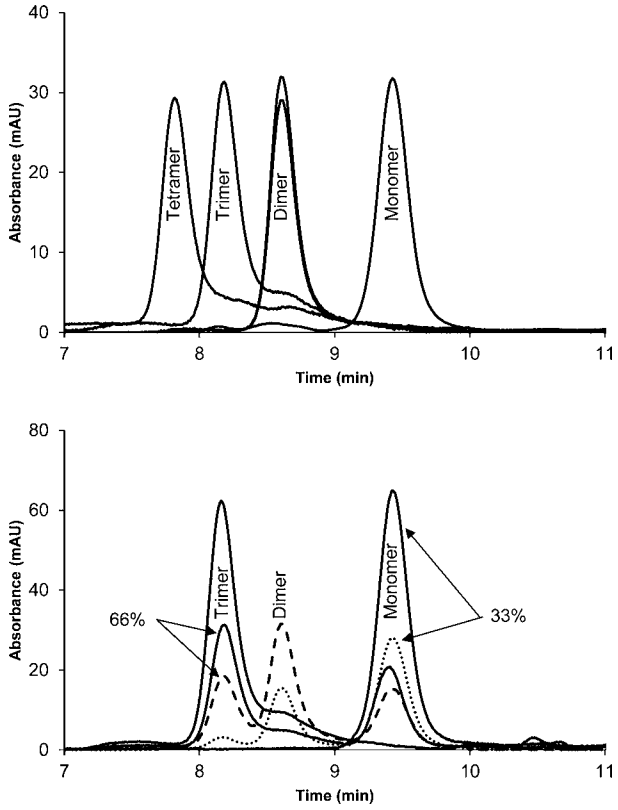

Figure 3. SEC−HPLC chromatograms of monomer units and stoichiometric assemblies on DNA1, DNA2, DNA3, and DNA4 (top panel) and during titration of monomer units with DNA3 (bottom panel). Forms eluted at 9.4 min (SNAP−PNA1−Atto488 monomer), 8.6 min (homodimer of SNAP−PNA1−Atto488:DNA1 and heterodimer of SNAP−PNA1−Atto488:SNAP−PNA3−Atto532:DNA2), 8.2 min (trimer of SNAP−PNA1−Atto488:DNA3), and 7.8 min (tetramer of SNAP−PNA1−Atto488:DNA4). During titration of SNAP−PNA1−Atto488 with DNA3, the elution times were unchanged. The observed distribution of products (solid lines in lower panel) did not match the distribution expected from the binomail distribution for either 33% (dotted line) or 66% (dashed line) saturation of sites on the DNA3 template. In both cases, there was an under-representation of the dimeric product relative to those expected on the basis of the binomial distribution. All of the chromatograms were obtained at the maximum absorption wavelength of Atto488 at 501 nm except for the heterodimer assembled on DNA2, which was at maximum absorption of Atto532 at 532 nm.

units separated by approximately 4.1 nm (0.64 R_0) with efficient energy transfer between donor and acceptor.

The estimated distance based on FRET (4.1 ± 0.2 nm) was within 2 SD of the computed distance (3.7 nm). The 3.7 nm estimate of the distance between Atto488 and Atto532 in the dimer assembly was based on summation of the lengths of the 4 bases in a GATC gap engineered between the complementary regions for PNA1 and PNA2, 6 PNA−DNA base pairs, and a lysine residue.[59] This accounted for the GATC gap and the structure of PNA−DNA double helices, which have 16 base pairs per turn with a 28° twist and 3.3 Å rise.[60] This distance (3.7 nm) also assumes that the two fluorophores in the 1:1:1 assembly are on the same side of the assembly. These considerations indicate excellent agreement between the FRET and computed distances and efficient formation of the heterotransfer assembly.

dx.doi.org/10.1021/bc500319p | Bioconjugate Chem. 2014, 25, 1820−1828

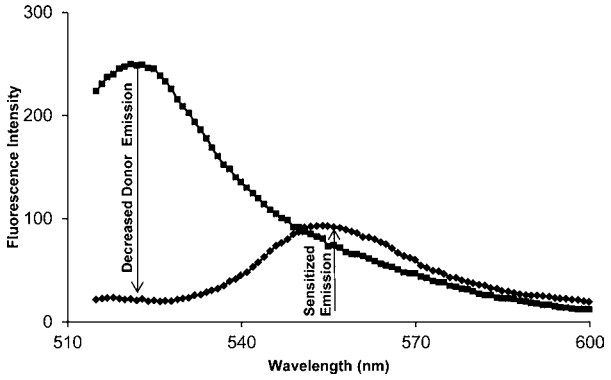

Figure 4. Uncorrected emission spectra of SNAP−PNA1−Atto488 when excited at 501 nm in the presence (♦) and absence (■) of acceptor. The emission intensity of SNAP−PNA1−Atto488 decreased after addition of an equimolar ratio of the acceptor (SNAP−PNA3−Atto532).

Homo-FRET System. Anisotropy Measurement of Homo-FRET System Indicating the Assembly in Dimer and Higher Oligomer Forms. A range of stoichiometries among DNA1, DNA3, and DNA4 were generated by varying the concentration of DNA (0 to 1 μM) in the presence of 1 μM SNAP−PNA1−Atto488 in order to study anisotropy changes upon assembly. In comparison to the measured anisotropy for SNAP−PNA1−Atto488 (monomer) (0.237 ± 0.002), the maximum anisotropy observed for each system was at 1:1 stoichiometry of DNA:monomer. The measured anisotropies of 1:1 stoichiometries for DNA1:SNAP−PNA1−Atto488, DNA3:SNAP−PNA1−Atto488, and DNA4:SNAP−PNA1−Atto488 were 0.26 ± 0.01, 0.27 ± 0.01, and 0.28 ± 0.03, respectively, which is in accord with a slight increase of rotational correlation time of the larger assemblies.

The anisotropy decreased as the complementary DNA became saturated with the PNA construct, confirming assemblies exhibited homo-FRET. Titration of SNAP−PNA1−Atto488 with DNA1 resulted in a gradual decrease of anisotropy compared to that for DNA1:monomer, which reached a minimum of 48% of the initial value at a 2:1 ratio of SNAP−PNA1−Atto488:DNA1. Because the distance between two complementary parts for SNAP−PNA1−Atto488 constructs on the DNA1 scaffold is less than the 0.8 R_0 for Atto488 in homotransfer (R_0 = 5 nm), eq 1 predicts 50% depolarization, which is very close to the measured decrease and in accordance with the hetero-FRET assembly.

In template-directed oligomer formation via DNA3, the anisotropy decreased by 62% at a 3:1 ratio of SNAP−PNA1−Atto488 to DNA3 (Figure 5, top panel). This value is close to the 66% decrease predicted by eq 4, with any discrepancy attributable to variation in the overall size of the complex. Equation 4 assumes there is no significant mass change that would affect the rotational correlation time. However, the mass of a 3:1 assembly will be higher than that of either free SNAP−PNA1−Atto488 or a 1:1 stoichiometry of SNAP−PNA1−Atto488:DNA3.

Similarly, the lowest anisotropy measured for tetrameric assemblies on DNA scaffolds (0.086 ± 0.004) was from the solution with a 4:1 ratio of SNAP−PNA−Atto488:DNA4 (Figure 5, bottom panel). This solution showed a 69% anisotropy decrease, which is slightly less than predicted 75% (eq 4). As with the 3:1 mixture, the discrepancy is likely due to

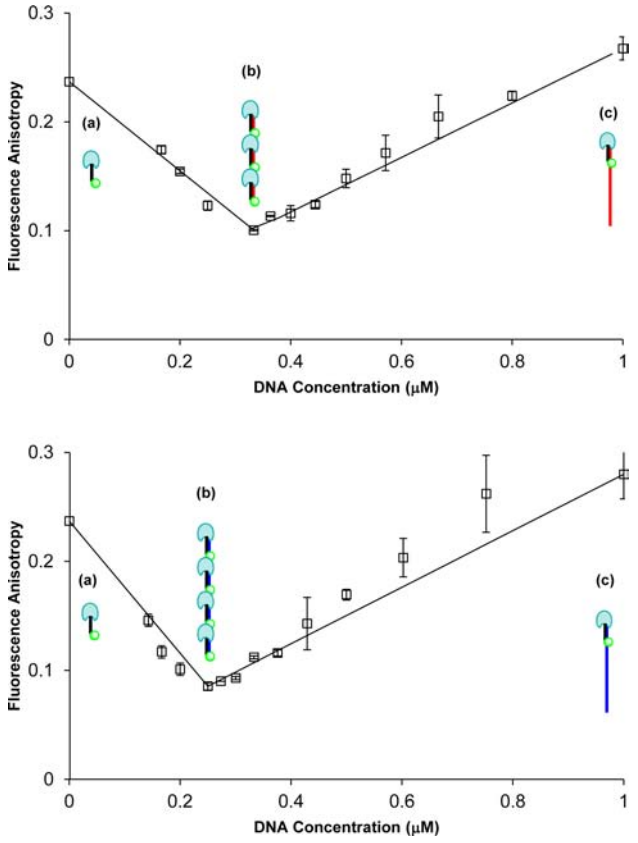

Figure 5. Anisotropy changes due to homo-FRET during titrations of SNAP−PNA−Atto488 with the DNA3 (upper panel) and DNA4 (lower panel) templates. The panels show the titration of 1 μM SNAP−PNA1−Atto488 with (0−1 μM) DNA3 and DNA4. The solid lines represent a kinetic/stoichiometric model (as opposed to stochastic models commonly applied in the literature) in which only the 1:1 and either the 3:1 (DNA3) or the 4:1 (DNA4) are present. Error bars are based on the standard deviations from two replicate measurements. In this model, the regions from (a) to (b) consist only of the free SNAP−PNA−Atto488 and the saturated form (e.g., 3:1 for DNA3 and 4:1 for DNA4), and the regions from (b) to (c) include only the 1:1 and the saturated form, with all templates forming the 1:1 product before proceeding to saturation (see Scheme 1).

the increase in mass in the 4:1 assembly relative to that of free SNAP−PNA1−Atto488 or 1:1 SNAP−PNA1−Atto488:DNA4.

In contrast to earlier work on a similar mTFP system,[5,57] none of the assemblies showed signs of quenching, indicating that the Atto488 dye satisfies the equal fluorescence efficiency assumption[61,62] in these assemblies. However, on the basis of the SEC-HPLC results, a stochastic model[57,61,62] was not warranted and a kinetic/stoichiometric model based on the considerations of Scheme 3 applied (Figure 5). In prior work on mTFP,[57] an adjustment was needed to account for reduced energy transfer between nonadjacent fluorophores, which was not required here. This suggests that the SNAP−Atto488 constructs have near ideal photophysics and that the BG constructs allow convenient labeling of proteins expressing the SNAP sequence, as illustrated by the template-directed assembly.

■ CONCLUSIONS

In summary, controllable assembly of fluorescent SNAP−PNA conjugates on DNA frameworks has been demonstrated. Taking advantage of the unique recognition capability of

dx.doi.org/10.1021/bc500319p | Bioconjugate Chem. 2014, 25, 1820−1828

PNA for complementary DNA scaffolds, the fluorescent SNAP−PNA units were precisely assembled in dimer and higher oligomer forms. The assemblies were characterized by HPLC, SDS-PAGE, and fluorescent techniques. Assemblies exhibiting either homo-FRET or hetero-FRET were created using DNA scaffolds, and distinct bands were observed in SEC-HPLC and SDS-PAGE for both intermediates and completed assemblies. Measurements of the anisotropy of homodimer and other homo-oligomers confirmed homo-FRET in the assemblies and, in combination with SEC-HPLC, suggested that a kinetic/stoichiometric rather than a stochastic model dominated the formation of these assemblies. It is anticipated that fluorescent and nonfluorescent SNAP−PNA will provide a useful tool to study hetero- and homo-oligomerization of any SNAP-tagged protein of interest either in vitro or in vivo. The ability to confirm assembly using FRET methods and potentially infer mechanistic aspects of assembly (stochastic vs kinetic/stoichiometric) should be especially valuable. Overall, the SNAP−PNA−fluorophore system presents a simple method to create arbitrary assemblies of any SNAP-enabled proteins in combination with homo-FRET, hetero-FRET, and multifluorophore-FRET.

Fluorescently labeled SNAP-tags have been widely used as markers for visualization of cell membrane protein clusters using FRET combined with fluorescence microscopy.[46,63] These systems for template-directed assembly were designed to investigate the assembly of cell membrane proteins (e.g., EGFR cluster formation and activation) by gaining external control of clustering in terms of size (dimer, trimer, etc.) and compositions (homo- and heteroaggregates). Although they have been tested with fluorophores attached, this is not a requirement. The template-directed assembly of labeled and unlabeled clusters of known size and composition applied in vivo may provide new insights into the mechanism of cell membrane protein activation via clustering, leading to new methods for regulation of signaling pathways that rely on biophysical and chemical inputs.

EXPERIMENTAL PROCEDURES

BG−PNA−Atto Dye Conjugation. The conjugation of BG−PNA was run on a 500 μL scale using a 1.5-fold excess of BG−maleimide (150 μM) (New England Biolabs, USA). The conjugation solution was 100 μM PNA1 (Cys-O-ACGTAC-Lys) or PNA2 (Cys-O-CAATGA-Lys) (PANAGENE, USA) in 500 μL of PBS buffer, pH 7.2, 150 μM freshly prepared BG−maleimide, and 1 mM of TCEP (Sigma-Aldrich) as a reducing agent. The mixture was incubated overnight at 4 °C. To achieve BG−PNA−Atto dyes, the coupling reactions were carried out by adding approximately 10 equiv of freshly prepared solutions of Atto488−NHS-ester and Atto532−NHS-ester (1 mM) (ATTO-TEC GmbH, Germany) to 200 μL of prepared BG−PNA1 and BG−PNA2 conjugates, respectively. The reaction mixture then incubated at room temperature for 2 h with shaking in the dark. Products were analyzed by MALDI-TOF MS and reverse-phase HPLC (RP-HPLC). The RP-HPLC was performed on a C-18 reverse-phase column eluted with a flow rate 1 mL/min with a 40 min linear gradient of acetonitrile/0.1% TFA started at 10−90%. Eluted compounds were detected with UV−visible absorbance.

Coupling Purified SNAP Protein to BG−PNA−Atto Dyes. Coupling was run on a 200 μL scale using a 2-fold excess of BG−PNA−Atto. The conjugation solution was 5 μM purified SNAP protein (New England Biolab, USA) in 200 μL of phosphate buffer, pH 7.4, 10 μM prepared BG−PNA1−Atto488 and BG−PNA2−Atto532, and 1 mM of TCEP as a reducing agent. The reaction mixture incubated for 2 h at 37 °C in the dark. Afterward, the final solution was purified by dialysis to remove unreacted compounds. These conditions were selected after evaluating the effects of temperature (37 °C and room temperature), different ratios of BG−PNA−Atto to SNAP (2- and 3-fold excesses), and different incubation times (2, 3, and 4 h) on the conjugation reaction while maintaining other conditions constant. The results of coupling were assessed by MALDI-TOF MS, SDS-PAGE, and size exclusion (SEC) HPLC. The SEC-HPLC was carried out on a size exclusion column (SRT SEC-150, 5 μm, 4.6 × 300 mm; Chromex Scientific, UK) calibrated with molecular weight protein marker kit 12−200 kDa (MWGF200, Sigma). The detection wavelengths were 214, 501 (maximum absorption wavelength of Atto488), and 532 nm (maximum absorption wavelength of Atto532).

Hybridization and Assembly of Fluorescent SNAP−PNA with DNA. Four DNA scaffolds (Life Technologies, USA) were used to hybridize to the fluorescent SNAP−PNA constructs. DNA1 (5′-TGCATGGATCTGCATG-3′) was used as a template to assemble two SNAP−PNA1−Atto488 constructs into a dimeric form. DNA2 (5′-TGCATGG-ATCGTTACT-3′) was applied to make heterodimer assemblies of SNAP−PNA1−Atto488 and SNAP−PNA3-Atto532. DNA3 (5′-TGCATGGATCTGCATGGATCTGCATG-3′) and DNA4 (5′-TGCATGGATCTGCATGGATCTG-CATGGATCTGCATG-3′) scaffolds were used to assemble SNAP−PNA1−Atto488 constructs in trimeric and tetrameric forms, respectively. The titration of 0.5 μM DNA1, 0.33 μM DNA3, and 0.25 μM DNA4 with different concentrations of SNAP−PNA1−Atto488 (0−1 μM) was carried out in phosphate buffer (100 mM, NaCl 200 mM, pH 7) with 2 h incubation at room temperature. The results were assessed by SDS-PAGE electrophoresis and SEC-HPLC at (214, 501, and 532 nm) as described in previous chapters. The SEC-HPLC calibrated with molecular weight protein marker kit 12−200 kDa (MWGF200-sigma).

Photophysical Measurements and Theory. Different concentrations of DNA1, DNA3, and DNA4 (0−1 μM) were added to 1 μM SNAP−PNA1−Atto488 in phosphate buffer (100 mM, NaCl 200 mM, pH 7) with 2 h incubation at room temperature. The anisotropy was recorded using a multimode microplate reader (Infinite F200 PRO, Tecan Group Ltd.). The excitation and emission wavelengths were 485 and 535 nm, respectively.

Similarly, 0.5 μM of SNAP−PNA1−Atto 488 and SNAP−PNA2−Atto532 were added to 1 μM DNA2. The intensity measurement was carried out using a fluorimeter (Cary Eclipse; Varian) over the range of 515−600 nm with excitation at 501 nm, which is the maximum absorption wavelength of Atto488.

Theory. Proximity between fluorescently labeled molecules may be assessed via FRET using either homo- or hetero-FRET methods. In homo-FRET studies, the fluorescence anisotropy is an indicator of energy transfer, and normally applied theories for assembly of two or more fluorophores into a cluster are based on the binomial distribution. This implies that when N binding sites exist on a species (S) and $\bar{i}$ is the average number of labeled sites, then the fraction, f_i, of the species in the form of SX_i ($0 \leq i \leq N$) is given by the binomial distribution

$$f_i = \binom{N}{i}\left(\frac{\bar{i}}{N}\right)^i\left(1 - \frac{\bar{i}}{N}\right)^{N-i} \quad (1)$$

This approach[61,62] allows the anisotropy of complex systems to be predicted when combined with the sum law of anisotropies if cluster formation does not affect the intensity of the fluorophores.[61,62,64,65]

$$r(f, N) = A_1 f^0 (1-f)^{N-1} r_1 + A_2 f(1-f)^{N-2} r_2 + \ldots + A_N f^{N-1}(1-f)^0 r_N \quad (2)$$

In this expression, f is the ensemble fractional labeling, A_1, A_2, ..., A_N are the values from the $N - 1$ row of Pascal's triangle, and r_1, r_2, ..., r_N are and fluorescence anisotropies of the N species. If interactions result in changes in the intensity of the fluorophores in the cluster, then a correction term, z_i, is required, yielding[57]

$$r(f, N) = \frac{\sum_{i=1}^{N} A_{i,N} z_i f^i (1-f)^{N-i} r_i}{\sum_{i=1}^{N} A_{i,N} z_i f^i (1-f)^{N-i}} \quad (3)$$

The anisotropies r_1, r_2, ..., r_N of the individual species in the mixture may be conveniently approximated when the interfluorophore distance is <0.8 R_0.[66] Under these conditions, if r_1 is the anisotropy of an assembly with one fluorophore and r_i is the anisotropy of a species with i fluorophores, then the individual anisotropies may be approximated.[66]

$$r_i = \frac{r_1}{i} \quad (4)$$

Depending on orientation, distance between fluorophores, and cluster size, this approximation may not hold rigorously, and additional considerations will be required.[66−68]

The binomial theory applies only when individual binding events are independent. As such, the treatments leading to eqs 1−3 assume the distribution of fluorophores is not affected by co-operative binding or other processes that might skew the distribution. For example, if the rate-limiting step in the assembly of PNA−X on a DNA template consisting of a motif with 3 repeats (Scheme 3) is k_2, with k_1 and k_3 fast, then the distribution of species in a substoichiometric reaction will favor the singly and triply labeled species.

Scheme 3

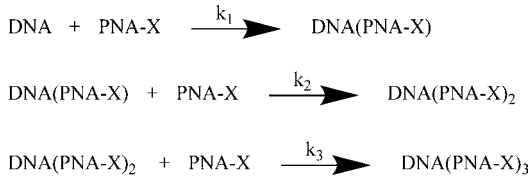

In these cases, f_i (when equal fluorescence efficiency occurs), f_i, and z_i (interactions enhance or quench fluorescence) or the fractional fluorescence intensity (ϕ_i) must be independently determined, and the sum law of anisotropies must be used directly.

$$r(N) = \sum_{i=1}^{N} \phi_i r_i \quad (5)$$

Verification of the validity of procedures based on stochastic assembly (e.g., binomial, Poisson, etc.)[62] may be done when separation of the individual species is possible.

AUTHOR INFORMATION

Corresponding Author

*E-mail: quentin.hanley@ntu.ac.uk.

Present Address

†(Z.G.) Puridify, Stevenage Bioscience Catalyst, SG1 2FX, United Kingdom.

Notes

The authors declare no competing financial interest.

ACKNOWLEDGMENTS

We acknowledge funding from NanoSci-E+ to the Nano-Actuate consortium. In the UK, NanoActuate was administered by EPSRC as EP/H00694X/1.

REFERENCES

(1) Niemeyer, C. M. (2010) Semisynthetic DNA−protein conjugates for biosensing and nanofabrication. *Angew. Chem., Int. Ed. 49*, 1200−1216.

(2) Niemeyer, C. M. (2004) Semi-synthetic DNA−protein conjugates: novel tools in analytics and nanobiotechnology. *Biochem. Soc. 32*, 51−3.

(3) Lu, H., Schops, O., Woggon, U., and Niemeyer, C. M. (2008) Self-assembled donor comprising quantum dots and fluorescent proteins for long-range fluorescence resonance energy transfer. *J. Am. Chem. Soc. 130*, 4815−4827.

(4) Prencipe, G., Maiorana, S., Verderio, P., Colombo, M., Fermo, P., Caneva, E., Prosperi, D., and Licandro, E. (2009) Magnetic peptide nucleic acids for DNA targeting. *Chem. Commun. 40*, 6017−6019.

(5) Gholami, Z., Brunsveld, L., and Hanley, Q. (2013) PNA-induced assembly of fluorescent proteins using DNA as a framework. *Bioconjugate Chem. 24*, 1378−1386.

(6) Rothemund, P. W. K. (2006) Folding DNA to create nanoscale shapes and patterns. *Nature 440*, 297−302.

(7) Pianowski, Z. L., and Winssinger, N. (2008) Nucleic acid encoding to program self-assembly in chemical biology. *Chem. Soc. Rev. 37*, 1330−1336.

(8) Rothlingshofer, M., Gorska, K., and Winssinger, N. (2011) Nucleic acid-templated energy transfer leading to a photorelease reaction and its application to a system displaying a nonlinear response. *J. Am. Chem. Soc. 133*, 18110−18113.

(9) Sadhu, K. K., Röthlingshöfer, M., and Winssinger, N. (2013) DNA as a platform to program assemblies with emerging functions in chemical biology. *Isr. J. Chem. 53*, 75−86.

(10) Seeman, N. C. (2003) DNA in a material world. *Nature 421*, 427−31.

(11) Feldkamp, U., and Niemeyer, C. M. (2006) Rational design of DNA nanoarchitectures. *Angew. Chem., Int. Ed. 45*, 1856−1876.

(12) Dadon, Z., Samiappan, M., Safranchik, E. Y., and Ashkenasy, G. (2010) Light-induced peptide replication controls logic operations in small networks. *Chem.—Eur. J. 16*, 12096−12099.

(13) Lo, P. K., Metera, K. L., and Sleiman, H. F. (2010) Self-assembly of three-dimensional DNA nanostructures and potential biological applications. *Curr. Opin. Chem. Biol. 14*, 597−607.

(14) Niemeyer, C. M. (2001) Nanoparticles, proteins, and nucleic acids: biotechnology meets materials science. *Angew. Chem., Int. Ed. 40*, 4128−4158.

(15) Roloff, A., and Seitz, O. (2013) Bioorthogonal reactions challenged: DNA templated native chemical ligation during PCR. *Chem. Sci. 4*, 432−436.

(16) Rozners, E. (2012) Recent advances in chemical modification of peptide nucleic acids. *J. Nucleic Acids 2012*, 8.

(17) Chakrabarti, R., and Klibanov, A. M. (2003) Nanocrystals modified with peptide nucleic acids (PNAs) for selective self-assembly and DNA detection. *J. Am. Chem. Soc. 125*, 12531−12540.

(18) Daguer, J. P., Ciobanu, M., Alvarez, S., Barluenga, S., and Winssinger, N. (2011) DNA-templated combinatorial assembly of

small molecule fragments amenable to selection/amplification cycles. *Chem. Sci. 2*, 625−632.
(19) Harris, J. L., and Winssinger, N. (2005) PNA Encoding (PNA=peptide nucleic acid): from solution-based libraries to organized microarrays. *Chem.—Eur. J. 11*, 6792−6801.
(20) Huang, K.-T., Gorska, K., Alvarez, S., Barluenga, S., and Winssinger, N. (2011) Combinatorial self-assembly of glycan fragments into microarrays. *ChemBioChem 12*, 56−60.
(21) Diaz-Mochon, J. J., Bialy, L., and Bradley, M. (2006) Dual colour, microarray-based, analysis of 10 000 protease substrates. *Chem. Commun. 0*, 3984−3986.
(22) Svensen, N., Díaz-Mochón, J. J., and Bradley, M. (2011) Decoding a PNA encoded peptide library by PCR: the discovery of new cell surface receptor ligands. *Chem. Biol. 18*, 1284−1289.
(23) Pouchain, D., Diaz-Mochon, J. J., Bialy, L., and Bradley, M. (2007) A 10,000 member PNA-encoded peptide library for profiling tyrosine kinases. *ACS Chem. Biol. 2*, 810−818.
(24) Lovrinovic, M., Seidel, R., Wacker, R., Schroeder, H., Seitz, O., Engelhard, M., Goody, R. S., and Niemeyer, C. M. (2003) Synthesis of protein-nucleic acid conjugates by expressed protein ligation. *Chem. Commun. 7*, 822−823.
(25) Kazane, S. A., Axup, J. Y., Kim, C. H., Ciobanu, M., Wold, E. D., Barluenga, S., Hutchins, B. A., Schultz, P. G., Winssinger, N., and Smider, V. V. (2013) Self-assembled antibody multimers through peptide nucleic acid conjugation. *J. Am. Chem. Soc. 135*, 340−346.
(26) Urbina, H. D., Debaene, F., Jost, B., Bole-Feysot, C., Mason, D. E., Kuzmic, P., Harris, J. L., and Winssinger, N. (2006) Self-assembled small-molecule microarrays for protease screening and profiling. *ChemBioChem 7*, 1790−1797.
(27) Winssinger, N. (2012) DNA display of PNA-tagged ligands: a versatile strategy to screen libraries and control geometry of multidentate ligands. *Artif. DNA 3*, 105−108.
(28) Hutchins, B. M., Kazane, S. A., Staflin, K., Forsyth, J. S., Felding-Habermann, B., Schultz, P. G., and Smider, V. V. (2011) Site-specific coupling and sterically controlled formation of multimeric antibody Fab fragments with unnatural amino acids. *J. Mol. Biol. 406*, 595−603.
(29) Gorska, K., Huang, K.-T., Chaloin, O., and Winssinger, N. (2009) DNA-templated homo- and heterodimerization of peptide nucleic acid encoded oligosaccharides that mimick the carbohydrate epitope of HIV. *Angew. Chem., Int. Ed. 48*, 7695−7700.
(30) Scheibe, C., Bujotzek, A., Dernedde, J., Weber, M., and Seitz, O. (2011) DNA-programmed spatial screening of carbohydrate-lectin interactions. *Chem. Sci. 2*, 770−775.
(31) Scheibe, C., and Seitz, O. (2012) PNA−sugar conjugates as tools for the spatial screening of carbohydrate−lectin interactions. *Pure Appl. Chem.*, 77−85.
(32) Scheibe, C., Wedepohl, S., Riese, S. B., Dernedde, J., and Seitz, O. (2013) Carbohydrate−PNA and aptamer−PNA conjugates for the spatial screening of lectins and lectin assemblies. *ChemBioChem 14*, 236−250.
(33) Spinelli, N., Defrancq, E., and Morvan, F. (2013) Glycoclusters on oligonucleotide and PNA scaffolds: synthesis and applications. *Chem. Soc. Rev. 42*, 4557−4573.
(34) O'Hare, H. M., Johnsson, K., and Gautier, A. (2007) Chemical probes shed light on protein function. *Curr. Opin. Struct. Biol. 17*, 488−494.
(35) Hinner, M. J., and Johnsson, K. (2010) How to obtain labeled proteins and what to do with them. *Curr. Opin. Biotechnol. 21*, 766−776.
(36) Juillerat, A., Heinis, C., Sielaff, I., Barnikow, J., Jaccard, H., Kunz, B., Terskikh, A., and Johnsson, K. (2005) Engineering substrate specificity of O6-alkylguanine-DNA alkyltransferase for specific protein labeling in living cells. *ChemBioChem 6*, 1263−1269.
(37) Johnsson, N., and Johnsson, K. (2007) Chemical tools for biomolecular imaging. *ACS Chem. Biol. 2*, 31−38.
(38) Johnsson, K. (2009) Visualizing biochemical activities in living cells. *Nat. Chem. Biol. 5*, 63−65.
(39) Keppler, A., Gendreizig, S., Gronemeyer, T., Pick, H., Vogel, H., and Johnsson, K. (2003) A general method for the covalent labeling of fusion proteins with small molecules in vivo. *Nat. Biotechnol. 21*, 86−89.
(40) Keppler, A., Pick, H., Arrivoli, C., Vogel, H., and Johnsson, K. (2004) Labeling of fusion proteins with synthetic fluorophores in live cells. *Proc. Natl. Acad. Sci. U.S.A. 101*, 9955−9959.
(41) Keppler, A., Arrivoli, C., Sironi, L., and Ellenberg, J. (2006) Fluorophores for live cell imaging of AGT fusion proteins across the visible spectrum. *Biotechniques 41*, 167−70.
(42) Keppler, A., Kindermann, M., Gendreizig, S., Pick, H., Vogel, H., and Johnsson, K. (2004) Labeling of fusion proteins of O6-alkylguanine-DNA alkyltransferase with small molecules in vivo and in vitro. *Methods 32*, 437−444.
(43) Lin, M. Z., and Wang, L. (2008) Selective labeling of proteins with chemical probes in living cells. *Physiology 23*, 131−141.
(44) Jung, D., Min, K., Jung, J., Jang, W., and Kwon, Y. (2013) Chemical biology-based approaches on fluorescent labeling of proteins in live cells. *Mol. BioSyst. 9*, 862−872.
(45) Gronemeyer, T., Chidley, C., Juillerat, A., Heinis, C., and Johnsson, K. (2006) Directed evolution of O6-alkylguanine-DNA alkyltransferase for applications in protein labeling. *Protein Eng., Des. Sel. 19*, 309−316.
(46) Komatsu, T., Johnsson, K., Okuno, H., Bito, H., Inoue, T., Nagano, T., and Urano, Y. (2011) Real-time measurements of protein dynamics using fluorescence activation-coupled protein labeling method. *J. Am. Chem. Soc. 133*, 6745−6751.
(47) Maurel, D., Banala, S., Laroche, T., and Johnsson, K. (2010) Photoactivatable and photoconvertible fluorescent probes for protein labeling. *ACS Chem. Biol. 5*, 507−516.
(48) Campos, C., Kamiya, M., Banala, S., Johnsson, K., and González-Gaitán, M. (2011) Labelling cell structures and tracking cell lineage in zebrafish using SNAP-tag. *Dev. Dyn. 240*, 820−827.
(49) Brun, M. A., Tan, K.-T., Nakata, E., Hinner, M. J., and Johnsson, K. (2009) Semisynthetic fluorescent sensor proteins based on self-labeling protein tags. *J. Am. Chem. Soc. 131*, 5873−5884.
(50) Donovan, C., and Bramkamp, M. (2009) Characterization and subcellular localization of a bacterial flotillin homologue. *Microbiology 155*, 1786−1799.
(51) Hussain, A. F., Kampmeier, F., von Felbert, V., Merk, H. F., Tur, M. K., and Barth, S. (2011) SNAP-tag technology mediates site specific conjugation of antibody fragments with a photosensitizer and improves target specific phototoxicity in tumor cells. *Bioconjugate Chem. 22*, 2487−2495.
(52) Kampmeier, F., Ribbert, M., Nachreiner, T., Dembski, S., Beaufils, F., Brecht, A., and Barth, S. (2009) Site-specific, covalent labeling of recombinant antibody fragments via fusion to an engineered version of 6-O-alkylguanine DNA alkyltransferase. *Bioconjugate Chem. 20*, 1010−1015.
(53) Bannwarth, M., Corrêa, I. R., Sztretye, M., Pouvreau, S., Fellay, C., Aebischer, A., Royer, L., Ríos, E., and Johnsson, K. (2009) Indo-1 derivatives for local calcium sensing. *ACS Chem. Biol. 4*, 179−190.
(54) Kamiya, M., and Johnsson, K. (2010) Localizable and highly sensitive calcium indicator based on a BODIPY fluorophore. *Anal. Chem. 82*, 6472−6479.
(55) Haruki, H., Gonzalez, M. R., and Johnsson, K. (2012) Exploiting ligand−protein conjugates to monitor ligand−receptor interactions. *PLoS One 7*, e37598.
(56) Pin, J. P., Comps-Agrar, L., Maurel, D., Monnier, C., Rives, M. L., Trinquet, E., Kniazeff, J., Rondard, P., and Prézeau, L. (2009) G-protein-coupled receptor oligomers: two or more for what? Lessons from mGlu and GABAB receptors. *J. Physiol. 587*, 5337−5344.
(57) Zolmajd-Haghighi, Z., and Hanley, Q. (2014) When one plus one does not equal two: fluorescence anisotropy in aggregates and multiply labeled proteins. *Biophys. J. 106*, 1457−1466.
(58) Hermanson, G. T. (2008) *Bioconjugate Techniques*, 2nd ed., Academic Press, Boston, MA.
(59) Carrion-Vazquez, M., Oberhauser, A. F., Fisher, T. E., Marszalek, P. E., Li, H., and Fernandez, J. M. (2000) Mechanical design of proteins studied by single-molecule force spectroscopy and protein engineering. *Prog. Biophys. Mol. Biol. 74*, 63−91.

(60) Menchise, V., De Simone, G., Tedeschi, T., Corradini, R., Sforza, S., Marchelli, R., Capasso, D., Saviano, M., and Pedone, C. (2003) Insights into peptide nucleic acid (PNA) structural features: the crystal structure of a D-lysine-based chiral PNA–DNA duplex. *Proc. Natl. Acad. Sci. U.S.A. 100*, 12021–12026.
(61) Weber, G., and Daniel, E. (1966) Cooperative effects in binding by bovine serum albumin. II. The binding of 1-anilino-8-naphthalenesulfonate. Polarization of the ligand fluorescence and quenching of the protein fluorescence. *Biochemistry 5*, 1900–1907.
(62) Yeow, E. K. L., and Clayton, A. H. A. (2007) Enumeration of oligomerization states of membrane proteins in living cells by Homo-FRET spectroscopy and microscopy: theory and application. *Biophys. J. 92*, 3098–3104.
(63) Sun, X., Zhang, A., Baker, B., Sun, L., Howard, A., Buswell, J., Maurel, D., Masharina, A., Johnsson, K., and Noren, C. J. (2011) Development of SNAP-tag fluorogenic probes for wash-free fluorescence imaging. *ChemBioChem 12*, 2217–2226.
(64) Weber, G. (1952) Polarization of the fluorescence of macromolecules. I. Theory and experimental method. *Biochem. J. 51*, 145–155.
(65) Lakowicz, J. R. (2006) *Principles of Fluorescence Spectroscopy*, Springer, New York.
(66) Runnels, L. W., and Scarlata, S. F. (1995) Theory and application of fluorescence homotransfer to melittin oligomerization. *Biophys. J. 69*, 1569–1583.
(67) Gautier, I., Tramier, M., Durieux, C., Coppey, J., Pansu, R. B., Nicolas, J. C., Kemnitz, K., and Coppey-Moisan, M. (2001) Homo-FRET microscopy in living cells to measure monomer–dimer transition of GFP-tagged proteins. *Biophys. J. 80*, 3000–3008.
(68) Bader, A. N., Hoetzl, S., Hofman, E. G., Voortman, J., van Bergen en Henegouwen, P. M. P., van Meer, G., and Gerritsen, H. C. (2011) Homo-FRET Imaging as a tool to quantify protein and lipid clustering. *ChemPhysChem 12*, 475–483.